

D R A F T

A Letter of Intent to the Jefferson Lab PAC43

Search for Gluonic Excitations of Light Quark Baryons with CLAS12 and the Forward Tagger in Hall B

A. D'Angelo,^{1,2} V. Burkert,³ S. Capstick,⁴ G. Fedotov,⁵ E. Golovach,⁵ R. Gothe,⁶ L. Lanza,²
V. Mokeev,³ A. Rizzo,² J. Ryckebusch,⁷ I. Skorodumina,^{5,6} M. Ungaro,³ and V. Ziegler³

¹*INFN, Sezione di Roma Tor Vergata, 00133 Rome, Italy*

²*Universita' di Roma Tor Vergata, 00133 Rome Italy*

³*Thomas Jefferson National Accelerator Facility, Newport News, Virginia 23606, USA*

⁴*Florida State University, Tallahassee, Florida 32306, USA*

⁵*Skobeltsyn Institute of Nuclear Physics, Lomonosov Moscow State University, 119234 Moscow, Russia*

⁶*University of South Carolina, Columbia, South Carolina 29208, USA*

⁷*Gent University, Gent, Netherland*

(Dated: April 18, 2015)

We express the intent of submitting a proposal to an upcoming Jefferson Lab program Advisory Committee to launch an experimental program that will utilize the CLAS12 detector system in Hall B augmented by the Forward Tagger (FT) with the goal of studying the s-channel excitation of baryons with substantial gluonic excitation strength (hybrid baryons). The experiment will use electron beams with energies of 6.6, 8.8 and 11 GeV impinging on a liquid hydrogen target placed in the CLAS12 center. Scattered electrons will be detected in an angle range of 2.5 to 4.5 degrees by detecting electromagnetic energy in the electromagnetic calorimeter that is part of the Forward Tagger covering a Q^2 range of 0.05–0.5 GeV². The virtual exchange photons will carry both a linear polarization as well a circular polarization (assuming the electron beam is polarized). Electrons scattered at polar angles greater than 6–7 degrees will be detected and reconstructed in the CLAS12 detector system using the High Threshold Cherenkov Counter (HTCC) and the sequence of pre-shower calorimeter (PCAL) and the electromagnetic calorimeter (EC). At the requested beam energies, the mass range $W < 4$ GeV will be covered. Due to the very high electron rate at the very forward polar angles, additional constraints on the hadronic final state will be built into the CLAS12 trigger system to reduce the recorded event rate to a maximum of 20KHz.

Contents

I. Introduction	2
II. Theoretical Studies	3
A. Model projections	3
B. Lattice QCD predictions	4
C. Hadronic couplings	4
D. Electromagnetic couplings	5
III. Experimental aspects	6
A. The CLAS12 detector	6
B. The Forward Tagger	7
C. Event Generators	7
D. Acceptance calculations	7
E. Expected event rates	7
IV. Data Analysis	9
A. Event selection	9
B. Partial wave analysis	10
C. Strategies for identifying Hybrid Baryons	11
V. Other topics in light quark baryon spectroscopy that are addressed with this LOI.	12
VI. Beamtime estimate	12
VII. Summary	13
References	13

I. INTRODUCTION

The ongoing program at Jefferson Lab and several other laboratories to study the excitation of nucleons in the so-called nucleon resonance region with real photon and with electron beams has been very successful. Although only a fraction of the data taken during the CLAS run groups g8, g9, g10, and g12 have been analyzed and published, the published data have allowed to make very significant advances in light-quark baryon spectroscopy, and led to strong evidence of several new nucleon excitations as listed in the PDG listing of 2014 [1]. These discoveries were possible due to the very high meson production rates possible in the energy-tagged photoproduction processes. Furthermore, the use of meson electroproduction has led to completely new insights into the nature of several prominent resonant baryons, e.g. the so-called Roper resonance $N(1440)\frac{1}{2}^+$. This state defied an explanation of its properties, such as mass, transition amplitudes and transition form factors within the constituent quark model (CQM). The analyses of the new electroproduction data was crucial in dissecting its complex structure and providing a qualitative and quantitative explanation of the space-time evolution of the state [3]. For example, the Roper was considered as a candidate for the lowest mass hybrid baryon [6]. It was only through the meson electroproduction data that this possibility could be dismissed [4, 5].

The theory of the strong interactions, QCD, not only allows for the existence of hybrid baryons, but Lattice QCD calculations now predict several baryon states with strong gluonic content, with the lowest mass hybrids approximately 1.3 GeV above the nucleon ground state of 0.94 GeV, i.e. in the range $W = 2.2 - 2.3$ GeV. In the meson sector, exotic states (hybrid mesons) are predicted with quantum numbers that cannot be obtained in pure $q\bar{q}$ configuration. The selection of mesons with such exotic quantum numbers provides a convenient way to identify candidates for gluonic mesons. In contrast to the meson sector gluonic baryons (hybrid baryons) have quantum numbers that are also populated by ordinary excited 3-quark states. Hybrid baryons can mix with ordinary 3-quark excited states or with dynamically generated states making the identification of gluonic baryons more difficult. An important question is therefore: How can we distinguish gluonic excitations of baryons from their ordinary quark excitations? Another question is the mass range in which we may expect hybrid baryons to occur.

Mapping out the nucleon spectrum and the excitation strengths of individual resonances is a powerful way to answer a central question of hadron physics: "What are the effective degrees of freedom as the excited states are probed at

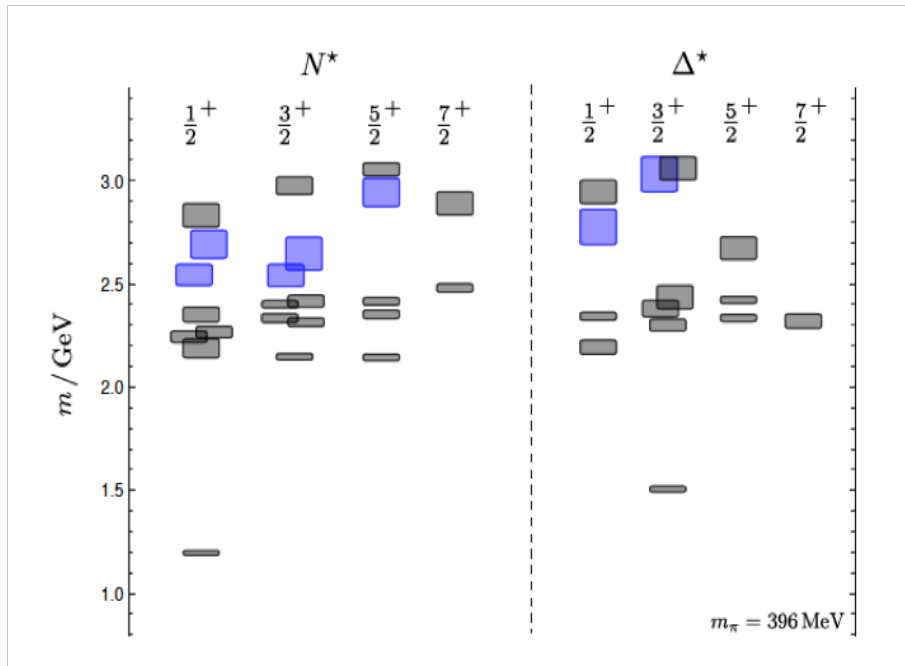


FIG. 1: The light-quark baryon spectrum predicted in Lattice QCD at a pion mass of 396 MeV. The blue shaded boxes indicate states with dominant gluonic excitations. Note that both the mass of the nucleon ground state and of the $\Delta(1232)$ are shifted by nearly 300 MeV to higher masses. This is largely due to the pion mass of 396 MeV.

different distance scales?”. Previous analyses of meson electroproduction have shown to be most effective in providing answers in several cases of excited states: $\Delta(1232)\frac{3}{2}^+$, $N(1440)\frac{1}{2}^+$, $N(1520)\frac{3}{2}^-$, $N(1535)\frac{1}{2}^-$, $N(1680)\frac{5}{2}^+$, $N(1675)\frac{5}{2}^-$. The experimental program outlined in this Letter-of-Intent is meant to vastly improve upon the available information and extend the reach of meson electroproduction to cover the full nucleon resonance mass range up to over 3.5 GeV and a larger Q^2 range. In conjunction with experiment E12-09-003, which focusses on the highest Q^2 , the proposed experiment will provide a complete program of nucleon resonance electroexcitation.

II. THEORETICAL STUDIES

A. Model projections

Gluonic excitations of the nucleon have been broadly discussed first in 1983 [6] in an extension of the MIT bag model to states where a constituent gluon in the lowest energy transverse electric mode combines with three quarks in a color octet state to form a colorless state in the mass range of 1.600 ± 0.100 GeV [4]. The glue flux-tube model applied to hybrid baryons [7, 8] came up with similar quantum numbers of the hybrid states, but predicted considerably higher masses than the bag model. For the lowest mass hybrid baryon a mass of 1.870 ± 0.100 GeV was found. In all cases the lowest mass hybrid baryon was predicted as a $J^P = 1/2^+$ state, i.e. a nucleon-like or Roper"-like state. Hybrid baryons were also discussed in the Large N_c approximation of QCD for heavy quarks [11], which also led to the justification of the constituent glue picture used in the models. The high energy behavior of hybrid baryons was discussed in [9]. However, in contrast to hybrid meson production, which has received great attention both in theory and in experiments, the perceived difficulties of isolating hybrid baryon states from ordinary quark states let this part of the field to remain dormant for a decade.

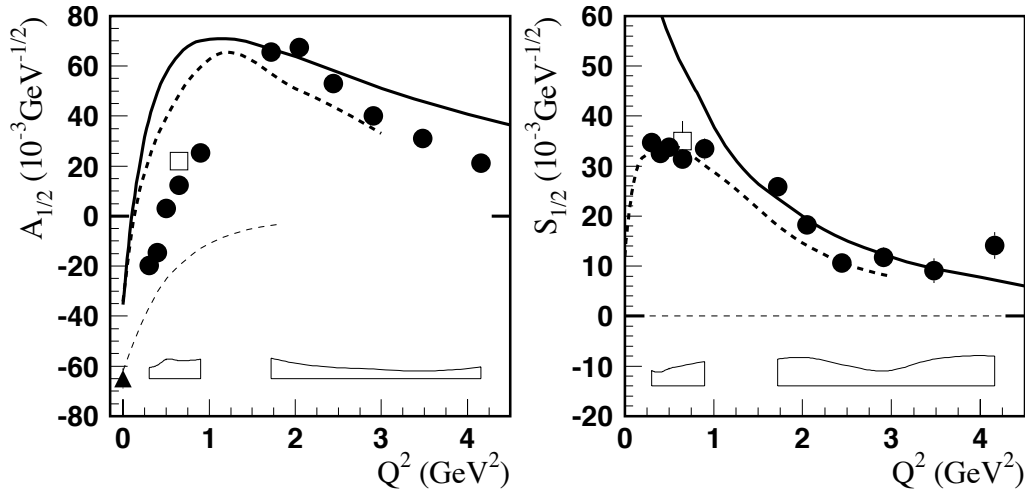


FIG. 2: Electrocoupling amplitudes of the Roper resonance $N(1440)_{\frac{1}{2}}^{+}$. The thin dashed lines are the constituent quark-gluon model predictions for the gluonic Roper.

B. Lattice QCD predictions

The first quenched calculations on the lattice came in 2003 [10], where the lowest gluonic excitation of the 3-quark system was projected at a mass of 1 GeV above the nucleon mass, placing the lowest hybrid baryon at a mass around 2 GeV. The first LQCD calculation of the full light-quark baryon spectrum with unquenched quarks occurred in 2012 that included the projections of the hybrid nucleon N_G states and hybrid Δ_G states [12]. Figure 1 shows the projected light quark baryon spectrum in the lower mass range. At the pion mass of 396 MeV used in this projection, the prediction for the lowest hybrid nucleon $J^P = \frac{1}{2}^{+}$ state, gives a mass of about 1.3 GeV above the nucleon ground state, i.e. in a mass range of 2.2 - 2.3 GeV (note that in this calculation the nucleon mass is shifted by nearly 300 MeV to higher masses). In the following we take this shift into account by subtracting 300 MeV from the masses of excited states in Fig. 1. As stated in [12], the lowest hybrid baryons, shown in Fig. 1 in blue, were identified as states with leading gluonic excitations. If hybrid baryons are not too wide, we might expect the lowest hybrid baryon to occur in a mass range of 2.2 - 2.3 GeV, a few hundred MeV above the band of radially excited $J^P = \frac{1}{2}^{+}$ 3-quark nucleon excitations of isospin $\frac{1}{2}$ and thus possibly well separated from other states. In this computation the lowest $J^P = \frac{3}{2}^{+}$ gluonic states are nearly mass degenerate with the corresponding $J^P = \frac{1}{2}^{+}$ gluonic states generating a glue-rich mass range of hybrid nucleons. If these projections hold up with LQCD calculations using near physical pion masses, one should expect a band of the lowest mass hybrid baryon states with spin-parity $\frac{1}{2}^{+}$ and $\frac{3}{2}^{+}$ to populate a relatively narrow mass band of 2.2 - 2.5 GeV. Note, that these states fall into a mass range where no excited quark nucleon states are predicted to exist from these calculations. The corresponding negative parity hybrid states are expected to occur at much higher masses and are not included in this graph, and are not further considered here, although they may be subject of analysis should they appear within the kinematics covered by this LoI.

C. Hadronic couplings

Very little is known about possible hadronic couplings of hybrid baryons. One might expect an important role for final states with significant gluonic content, e.g. $B_G \rightarrow N\eta'$, or final states containing $s\bar{s}$ contributions due to the coupling $G \rightarrow s\bar{s}$, e.g. $B_G \rightarrow K^+\Lambda$, $B_G \rightarrow N^*(1535)\pi \rightarrow N\eta\pi$, $B_G \rightarrow N\pi\pi$, $B_G \rightarrow \phi(1020)N$ and $B_G \rightarrow K^*\Lambda$. Quark-model estimates of the hadronic couplings would be helpful in selecting the most promising final state for the experimental evaluation. As long as such estimates are not available we will use a range of assumptions on the hadronic couplings to estimate the sensitivity required for definitive measurements. Assuming hadronic couplings of a few % in the less complex final states, e.g. $K^+\Lambda$, $K^*\Lambda$, or $N\pi\pi$ we should be able to identify these states and proceed to establish their electromagnetic couplings and Q^2 dependence.

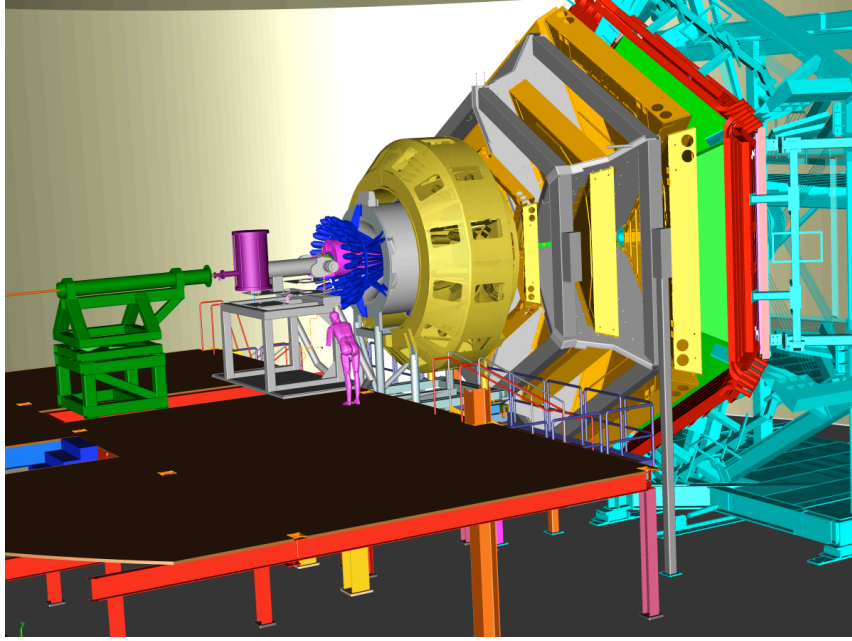


FIG. 3: The CLAS12 detector.

D. Electromagnetic couplings

Electromagnetic couplings have been studied within a non-relativistic constituent quark-gluon model and only for two possible hybrid states, the Roper $N_G(1440)\frac{1}{2}^+$ and the $\Delta_G(1600)\frac{3}{2}^+$. In reference [14] the photoexcitation of the hybrid Roper resonance $N(1440)\frac{1}{2}^+$ was studied, and in reference [15] the electroproduction transition form factors of a hybrid Roper state were evaluated. The latter was essential in eliminating the Roper resonance as a candidate for a hybrid state, both due to the transverse helicity amplitude and its Q^2 dependence and the prediction of $S_{1/2}(Q^2) = 0$ at all Q^2 . It also showed that a hybrid Roper transition amplitudes should behave like the ones of the ordinary $\Delta(1232)\frac{3}{2}^+$ for both its transition amplitudes. Recent measurements of the electrocoupling transition amplitudes are shown in Figure 2. Both amplitudes exhibit a Q^2 dependence that is distinctively different from the gluonic baryon prediction. Especially the scalar amplitude $S_{1/2}(Q^2)$ was found to be large while it is predicted to be equal zero in leading order.

The aforementioned predictions should apply to the lowest mass hybrid state with $J^P = \frac{1}{2}^+$. One may ask about the model-dependence of this prediction. The transverse amplitude has model sensitivity in its Q^2 dependence and depends on model ingredients, however, there are no quark model predictions that would come even close to the predictions of the hybrid quark-gluon model. The radial excitation of the Roper resonance gives a qualitatively different prediction for $A_{1/2}(Q^2)$ compared to the hybrid excitation, where the 3-quark component remains in the ground state with only a spin-flip occurring (just as for the $N - \Delta(1232)$ transition). The suppression of the longitudinal coupling, i.e. $S_{1/2}(Q^2) = 0$, is a property of the γqG vertex and is largely independent of specific model assumptions.

These studies have so far only been done for the two states $N(1440)\frac{1}{2}^+$ and $\Delta(1600)\frac{3}{2}^+$. The latter state was considered as a candidate for the lowest mass gluonic Δ_G . A result similar to the one for the hybrid Roper is found in [15] for a hybrid $\Delta_G(1600)\frac{3}{2}^+$, i.e. a fast falling $A_{1/2}(Q^2)$ and $S_{1/2}(Q^2) \approx 0$. The amplitudes at the photon point are not inconsistent with the quark model calculation but are inconsistent with the hybrid baryon hypothesis. This result is also in line with the expectation that the lowest mass hybrid states should have considerably higher masses than the first radially excited quark states. Note that there are currently no data for the Q^2 dependence of the $A_{1/2}$ and $S_{1/2}$ amplitudes of this state.

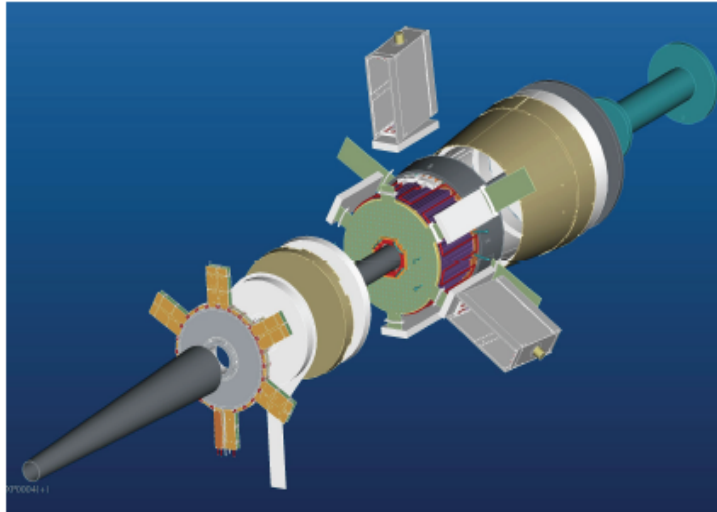


FIG. 4: The Forward Tagger (FT) system. The FT provides electron and high energy photon detection in a range of polar angles $\theta_e = 2.5^\circ - 4.5^\circ$, and will be fully integrated into the operation of CLAS12. Details on the specifications and expected operational performance may be obtained from <https://www.jlab.org/Hall-B/clas12-web/specs/ft.pdf>.

III. EXPERIMENTAL ASPECTS

A. The CLAS12 detector

The experimental program will use the CLAS12 detector shown in Fig. 3 for the detection of the hadronic final state. CLAS12 consists of a Forward Detector (FD) consisting of six symmetrically arranged sectors defined by the six coils of the toroidal superconducting magnet. Charged particle tracking is provided by a set of 18 drift chambers with a total of 36 layers in each sector. Additional tracking at $5^\circ - 35^\circ$ is due to a set of 6 layers of micromesh gas detectors (micromegas) immediately down stream of the target area and in front of the High-Threshold Cherenkov counter (HTCC). Particle identification is provided by time-of-flight information from two layers of time-of-flight detectors. Electron, photon and neutron detection are provided by the triple electromagnetic calorimeter, PCAL, EC(inner) and EC(outer). The heavy gas Cherenkov counter (LTCC) provides separation of high momentum pions from kaons and protons. The Central Detector (CD) consists of 6-8 layers of silicon strip detectors with stereo readout, 6 layers of micromegas, arranged as a barrel around the target, 48 scintillator bars to measure particle time-of-flight detector from the target (CTOF), and a central neutron detector. Further details on all CLAS12 components (magnets, detectors, data acquisition, software) may be obtained from: <https://www.jlab.org/Hall-B/clas12-web/>.

A polarized electron beam will be scattered off a liquid hydrogen target. The scattered electrons will be detected in the forward detectors of CLAS12 for scattering angle greater than about 6° . Momentum reconstruction will be done in the drift chamber system consisting of 36 layers of drift chambers, which are localized in 3 regions called R1, R2, and R3. Additionally, tracking will make use of the 6 layers of the forward micromegas tracker (FMT), which will improve vertex reconstruction and overall angle and momentum resolution. Electron identification uses the high threshold Cherenkov Counter (HTCC), the pre-shower calorimeter (PCAL), and the electromagnetic calorimeter (EC). Timing hits in the forward time-of-flight system (FTOF) will also be required. Electrons scattered at angles from $2.5^\circ - 4.5^\circ$ will be detected in the lead-tungstate calorimeter and the scintillation hodoscope and tracked in a double layer of micromegas tracker. The use of both the FT and CLAS12 to detect scattered electrons provides coverage in a wide range in Q^2 , from quasi-real photons at $Q^2 = 0.05 - 0.6 \text{ GeV}^2$ and at $Q^2 = 0.7$ to 10 GeV^2 . Charged hadrons will be measured in the full range from $6^\circ - 130^\circ$ with the polar angle acceptance depending somewhat on their charges. Detection of high-energy photons is possible for polar angles from $2.5^\circ - 35^\circ$ using the PCAL and EC as well as the FT calorimeter. At an operating luminosity of $L = 10^{35} \text{ cm}^{-2} \text{ s}^{-1}$ hadronic rates of $5 \times 10^6 \text{ s}^{-1}$ are expected.

B. The Forward Tagger

An essential component of the hadron spectroscopy program with CLAS12 is the Forward Tagger (FT) shown in Fig 4. The FT uses a high resolution crystal calorimeter composed of 324 lead-tungstate crystals to measure the scattered electrons in the polar angle range of 2.5° to 4.5° , and with full coverage in azimuthal angle. The calorimeter measures electron and photon energies with an energy resolution of $\sigma(E)/E \leq 0.02/\sqrt{E} \oplus 0.01$. The fine granularity of the calorimeter also provides good polar angle resolution. A 2-layer tiles scintillator hodoscope is located in front of the calorimeter for the discrimination of photons. A four-layer micromegas tracker will be used for precise electron tracking information. To discriminate charged and neutral particles two layers of a scintillator tiles hodoscope and four layers of a micromegas tracker are incorporated in front of the calorimeter. Electron detection in the FT will allow probing the crucial Q^2 range where hybrid baryons maybe identified due to their fast drop in the $A_{1/2}(Q^2)$ amplitude and the suppression of the scalar $S_{1/2}(Q^2)$ amplitude.

C. Event Generators

In order to have a realistic account of the acceptance for the processes we propose to study, two event generators were developed for the processes $ep \rightarrow e'K^+\Lambda$ and $ep \rightarrow e'p\pi^+\pi^-$, respectively.

The $ep \rightarrow e'K^+\Lambda$ event generators is based on model cross section calculations. The models [17] for $K^+\Lambda$ and [18] for $K^+\Sigma^0$ channels) describe KY electroproduction in the framework of a Regge-plus-resonance approach. Resonance contribution in s-channel is described with the help of effective-Lagrangian approach and the background part of the amplitude is modeled in terms of t-channel Regge-trajectory exchange. Comparison of a model cross section with the CLAS data is demonstrated in Fig. X - Fig. Y (**WE NEED THE FIGURES AS INPUT HERE**). The fully integrated cross section as a function of Q^2 is shown in Fig. 5. The accuracy of the model to reproduce available data in the range $0.65 \leq Q^2 \leq 2.55\text{GeV}^2$ and in the W range $1.6 \leq W \leq 2.2\text{GeV}$ is sufficient for the purpose of event generating. We rely on the model cross section at $Q^2 \leq 0.65\text{GeV}^2$.

WE NEED DESCRIPTION OF THE N-pi-pi EVENT GENERATOR

D. Acceptance calculations

Acceptance calculation were carried out using the CLAS12 FASTMC Monte Carlo, which uses a realistic parameterization of the polar and azimuthal angle and momentum acceptances of the CLAS12 detector system. It allows a fast simulation of the geometrical acceptances of CLAS12 using momentum-dependent able acceptances. For a fully realistic simulation the Geant4 based GEMC will be used for the development of a full proposal.

E. Expected event rates

At the very forward electron scattering angles, electron rates will be very high and exceed the nominal capabilities of the nominal data acquisition system event rates of 20KHz and 100MBsec^{-1} . Therefore additional constraints are needed to reduce the trigger rate to a few KHz. This requires the selection of a hadronic event pattern that should significantly enrich the sample with final state topologies as one might expect from hybrid baryon candidates. For realistic rate estimates, projections of hadronic coupling strengths of hybrid baryons are needed, which are currently not available. For an initial program we therefore consider to trigger on hadronic final states with at least two charged particle. This will cover final states: $K^+\Lambda \rightarrow K^+p\pi^-$, $p\pi^+\pi^-$, $p\phi \rightarrow pK^+K^-$, $p\eta' \rightarrow p\pi^+\pi^-\eta$. In addition, a single charged hadron trigger will be incorporated with a pre-scaling factor that will in parallel collect events with a single charged hadron in the final state, i.e. π^+n , $p\pi^0$, $K^+\Lambda$, and $K^+\Sigma$, among others.

The operating luminosity of CLAS12 is estimated at $L = 10^{35}\text{cm}^2\text{sec}^{-1}$. This corresponds to an event rate of 700 Hz (for $K^+\Lambda$) and about 500 Hz (for $K^+\Sigma^0$). For a 60 days run at that luminosity, the total number of $K^+\Lambda$ events is estimated at 3.7×10^9 , and the number of $K^+\Sigma$ events at 2.6×10^9 . The number of events in any histogram for certain smaller intervals of Q^2 and W , can be found in the same way. The lowest event rate is expected for high Q^2 and high W . For the kinematics with lowest statistics, e.g. $2.0 \leq Q^2 \leq 2.5\text{GeV}^2$ and $2.675 \leq W \leq 2.700\text{GeV}$, a total number of 4.0×10^5 $K^+\Lambda$ events, and 2.1×10^5 $K^+\Sigma^0$ events is expected.

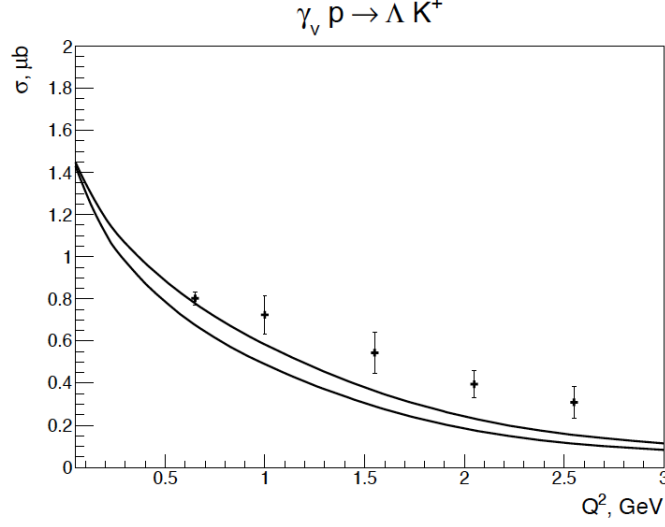


FIG. 5: Event generator compared with CLAS data for the integrated cross section.

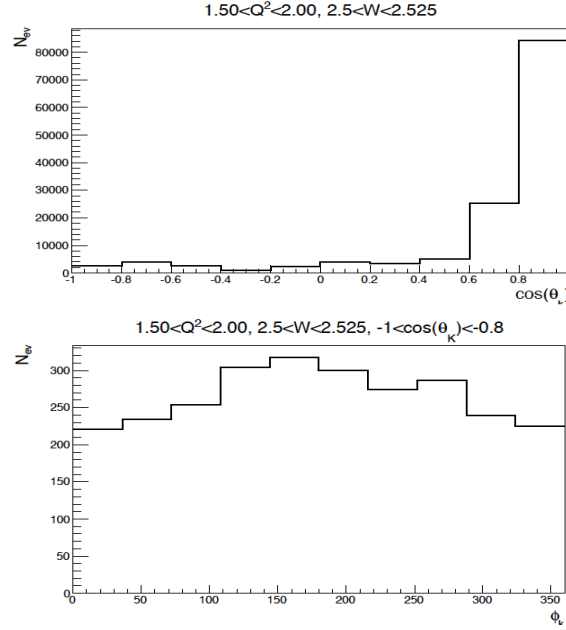


FIG. 6: Polar angle (top panel) and azimuthal angular distributions of simulated events for a specific kinematic bin in Q^2 and W . The forward peaking in the polar angle is due to the t -channel exchange contributions in the cross section.

While these rates seem very large, it should be kept in mind that the signals of hybrid baryons that we want to detect and quantify may be 10 times smaller than the signal from ordinary quark states and will likely not simply be seen as a peak in the excitation spectrum, but rather as a broad region in W where specific quantum numbers, i.e. $I = \frac{1}{2}$, $J^P = \frac{1}{2}^+$ or $J^P = \frac{3}{2}^+$ must be identified, and the electromagnetic couplings must be measured vs Q^2 . This can only be achieved in a partial-wave analysis that includes other channels into a multichannel fit, such as the Bonn-Gatchina or Jülich/GWU approaches. Very high statistics is thus essential, and the transverse and longitudinal

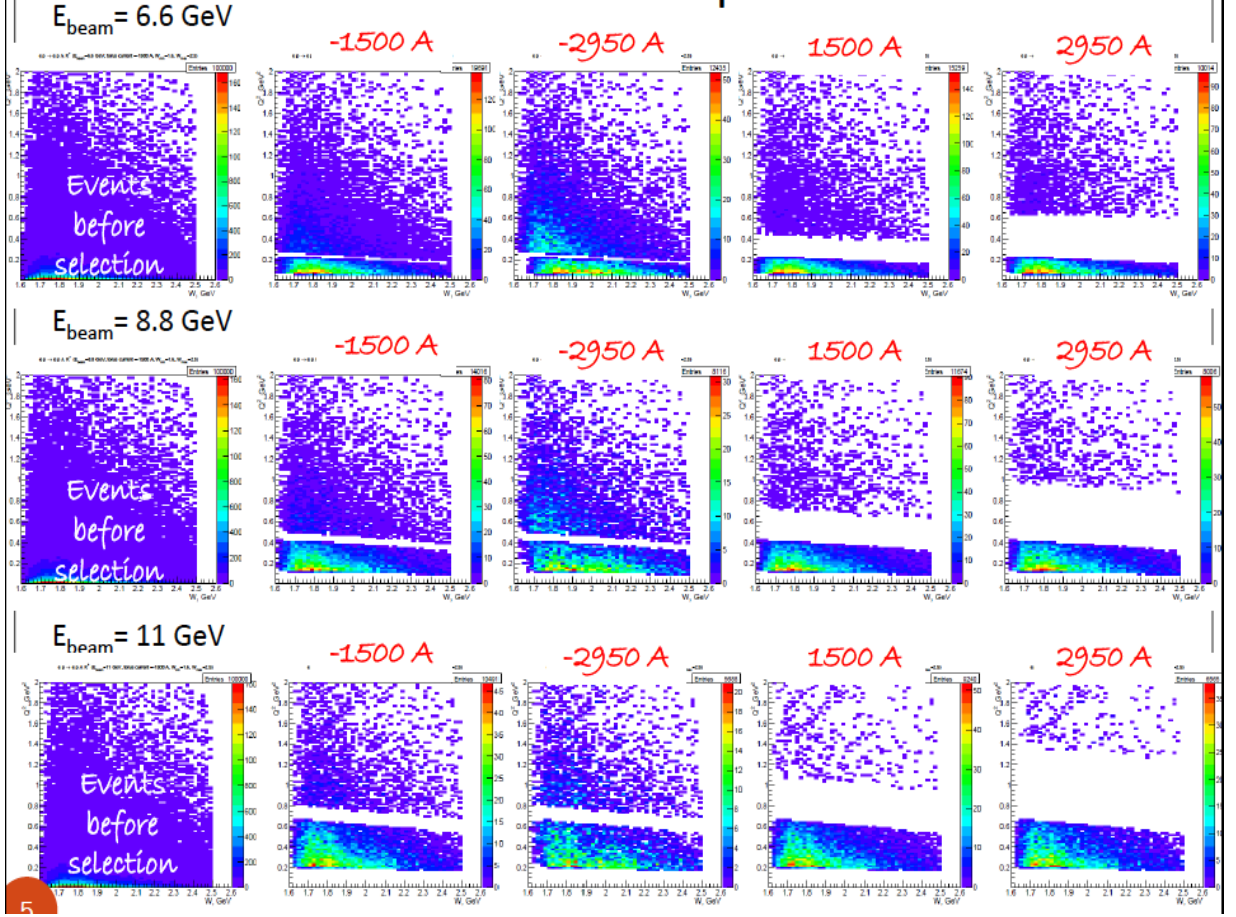


FIG. 7: Generated and accepted events in Q^2 and W , for beam energies of 6.6GeV, 8.8GeV,11.0GeV, and for different Torus currents 2950A and 1500A with positive and negative polarities. The wide bands in the acceptance are due to the gap between the accepted polar angle in the Forward Tagger and in CLAS12 proper. For outbending electrons in the Torus field the gap is small, while for inbending electrons the smallest accepted polar angle depends on the magnetic field strength and is increases with increasing magnetic field strength.

photon polarization that is inherent in electron scattering will provide the amplitude interference to enhance the resonant signal.

IV. DATA ANALYSIS

A. Event selection

Electrons will be detected both in the Forward Tagger and in the CLAS12 proper. In CLAS12 electrons can be identified at scattering angles above about 5 degrees in the high-threshold Cherenkov counter (HTCC) and in the PCA1 and EC calorimeters. Due to the higher Q^2 for electrons detected at larger scattering angles in CLAS12 compared to the FT region, the electron rate is comparatively much lower than the hadronic rate and good electron identification is important.

For electrons detected in the FT the low Q^2 leads to a very high electron rate that completely dominates the event rate in the FT calorimeter and hodoscope. A direct electron identification at the trigger level is not needed. However

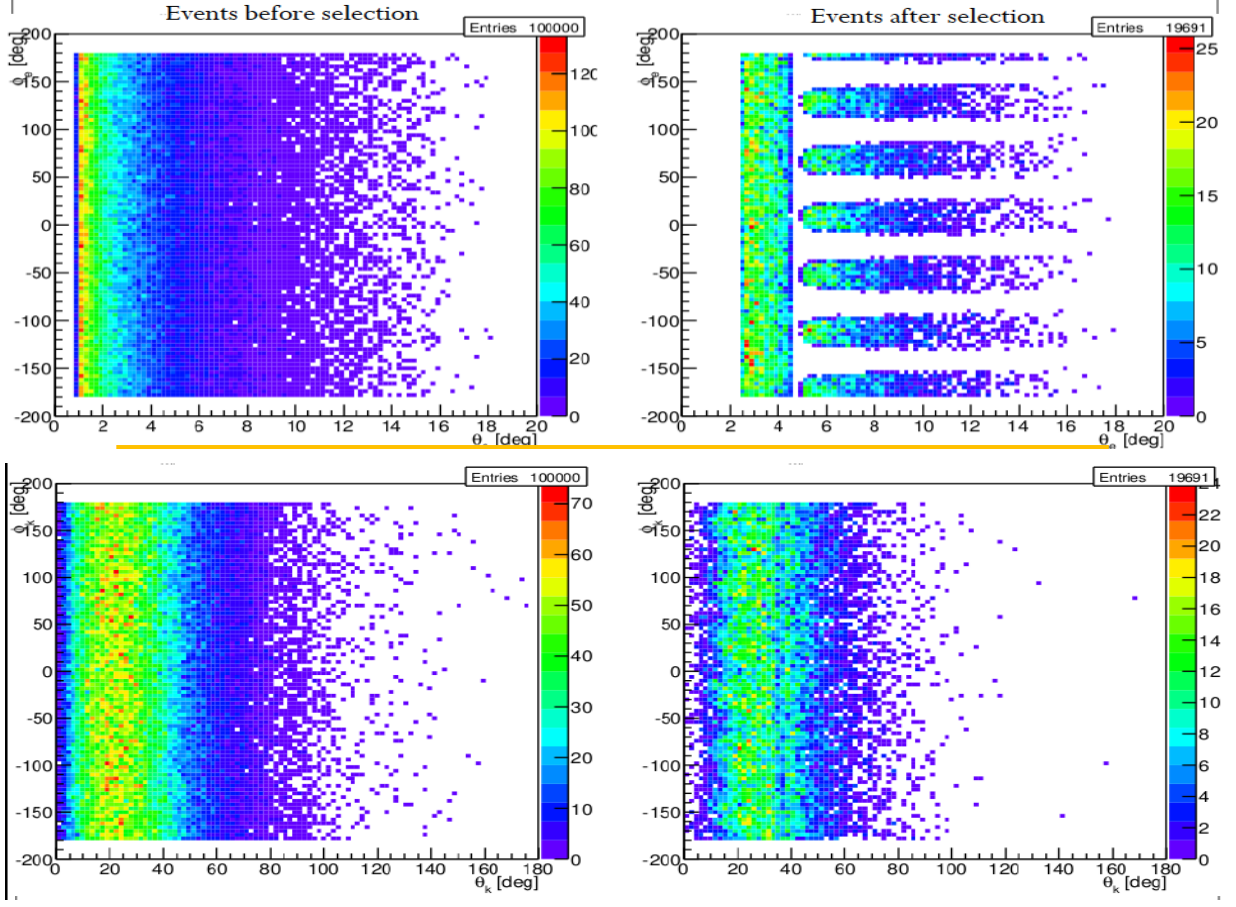


FIG. 8: Upper panels: Simulated scattered electrons (left), and accepted electrons (right). The bottom panels show the same distributions for the K^+ . Electrons are detected in the Forward Tagger in the full azimuthal angle ϕ and in the polar angle range θ_e for $2.5^\circ - 4.5^\circ$. In CLAS12 sectors azimuthal coverage is limited.

the complete event pattern may be checked for consistency with that hypothesis in the event reconstruction. Note that the full electron kinematics is measured in the FT calorimeter and the micromegas tracker and charged particle id is provided by the two layer hodoscope in front of the calorimeter.

Charged hadrons (π^\pm , K^\pm and protons) will be tracked in the drift chamber and micromegas and the silicon tracker and barrel micromegas at large angles, and identified in the CLAS12 time-of-flight detector system. Photons and neutrons are detected at forward angles in the electromagnetic calorimeters (PCAL, EC, FT) and neutrons at large angles in the central neutron detector (CDN).

B. Partial wave analysis

Using modern partial wave analyses tools several new excited N^* and Δ^* states have been identified or have been significantly improved in their evidence and star rating in the 12 edition of the Review of Particle Properties (RPP) of the particle Data Group [1] using the high statistics data in the photoproduction of a number of final states, e.g. $K^+\Lambda$, $K^+\Sigma$, 1^+n , $p\pi^0$, including polarization observables. This success has validated the importance of high statistics data sets in the search for new excited states, and has helped re-vitalized the field of hadron spectroscopy. In the analysis of the data to be taken with the proposed program discussed in this letter-of-intent we will make full use of

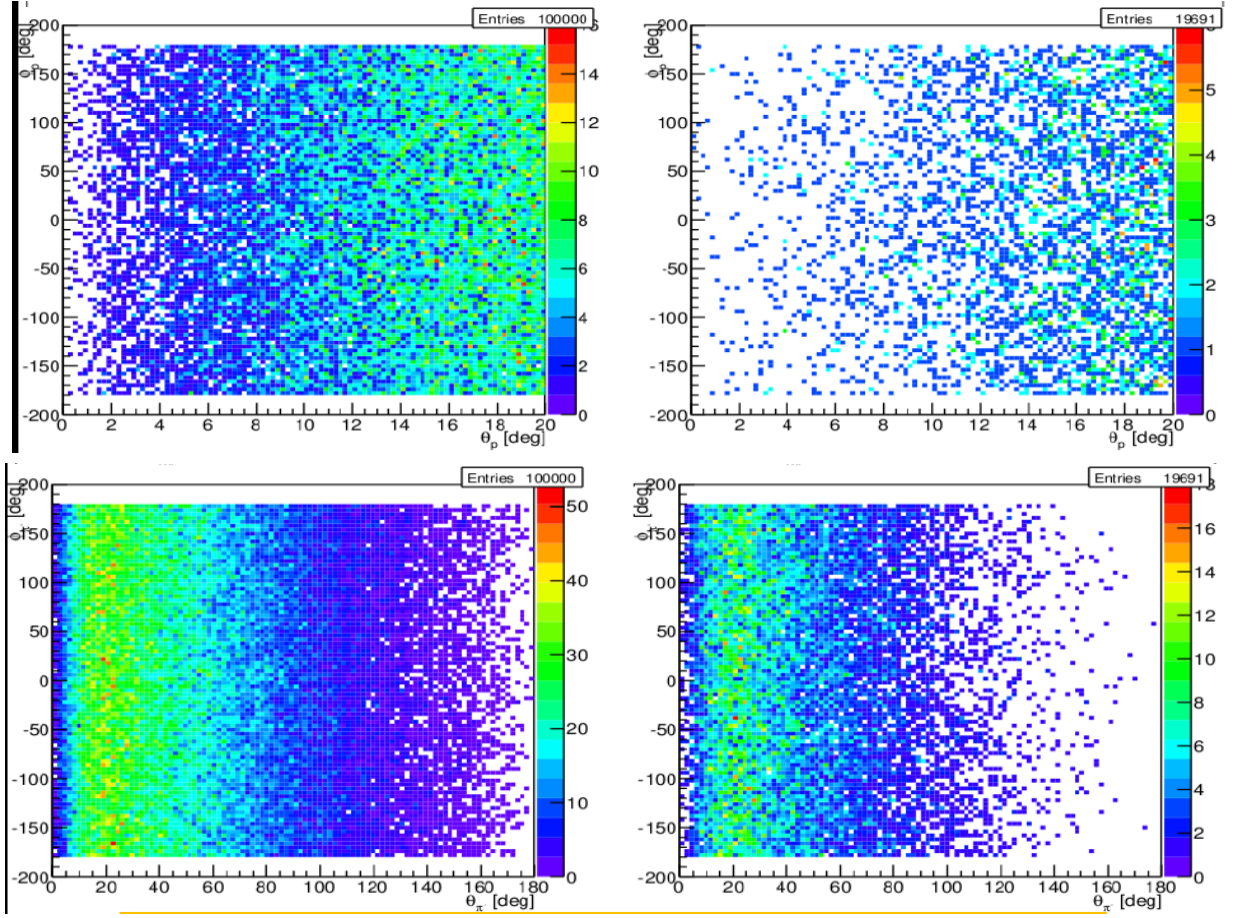


FIG. 9: Upper panels: Simulated proton distribution (left), and accepted protons (right). The bottom panels show the same distributions for the π^- . NOTE THAT THE ANGLE COVERAGE FOR PROTONS IS TRUNCATED!!!!

these advanced tools of amplitude analysis and partial wave analysis. Significant progress has also been made in the analysis of electroproduction data where transition form factors have been extracted from several excited states using the high statistics data from CLAS [4, 5, 16]. We feel strongly that these packages will be well-honed by the time the proposed data will be taken, including the extension of the photoproduction analysis to include the existing and planned electroproduction data sets.

C. Strategies for identifying Hybrid Baryons

In this section we address the question if and how gluonic hybrid baryons are distinct from ordinary quark excitations. As discussed in section II B the lowest hybrid baryons should have isospin $I = \frac{1}{2}$ and $J^P = \frac{1}{2}^+$ or $J^P = \frac{3}{2}^+$, and their masses should be in the range 2.20-2.50 GeV. This mass range must be verified once LQCD calculations with physical pion masses become available, as this range may shift with more realistic pion masses, likely to the lower mass range. Four states with $I = \frac{1}{2}$ and $J^P = \frac{1}{2}^+$ are projected with dominant quark excitations are predicted with masses below the mass of the projected hybrid states. Of these four states two are well the known $N(1440)\frac{1}{2}^+$, and $N(1710)\frac{1}{2}^+$, and two are the less well established $N(1880)\frac{1}{2}^+$ and $N(2100)\frac{1}{2}^+$ have 2* and 1* ratings, respectively. Another state $N(2300)$ has a 2* rating, and falls right into the lowest hybrid mass band projected by LQCD. Could

this state be the predicted lowest hybrid state?

In order to address this question, it is necessary to confirm (or refute) the existence of the 2^* state $N(1880)$ and the 1^* state $N(2100)$, as well as, measuring the electromagnetic couplings of $N(2300)$ and its Q^2 dependence. Improved information on the lower mass states should become available in the next one or two years when the new high-statistic single and double polarization CLAS data have been included into the multi-channel analyses frameworks, such as the Bonn-Gatchina or Jülich/GWU approaches. Should these two states be confirmed, then any new nucleon state with $J^P = \frac{1}{2}^+$ and in the right mass range, would be a candidate for the lowest mass hybrid baryon. The $N(2300)\frac{1}{2}^+$ state has been seen at BES III only in the invariant mass $M(p\pi^0)$ of $\Psi(2S) \rightarrow p\bar{p}\pi^0$ events. In this case the production of $N(2300)$ occurs at very short distances as it involves heavy quark flavor $c\bar{c}$ creation. Hence the state may be observable best in pion electroproduction $ep \rightarrow e'\pi^+n$ and $ep \rightarrow e'\pi^0p$ at high Q^2 , if its photocouplings amplitude is sufficiently strong to be measurable.

In the $J^P = \frac{3}{2}^+$ sector the situation is more involved. There are two hybrid states predicted in the mass range 2.2 to 2.4 GeV, with masses above five quark model states at same J^P . Of the five states, two are well known 4^* and 3^* states, $N(1720)\frac{3}{2}^+$ and $N(1900)\frac{3}{2}^+$, and one state, $N(2040)\frac{3}{2}^+$, has a 1^* rating. Here we will have to confirm (or refute) the 1^* star state and find two or three (if $N(2040)$ is not existing) more quark model state with same quantum numbers in the mass range 1.7 to 2.1 GeV.

The expected signature of the lowest mass hybrid baryons consist of:

- resonances with masses in the mass range $2.2 \leq W \leq 2.5\text{GeV}$ with $J^P = \frac{1}{2}^+$ or $J^P = \frac{3}{2}^+$
- a Q^2 dependence of the transverse helicity amplitude $A_{1/2}(Q^2)$ similar to the $\Delta(1232)\frac{3}{2}^+$.
- a strongly suppressed helicity amplitude $S_{1/2}(Q^2) \approx 0$ in comparison to other ordinary 3-quark states or meson-baryon excitations.

While these signatures maybe used to identify gluonic baryon excitations, the expected high statistics data will be used to identify any new or poorly known state whether or not it is a candidate for a hybrid baryon state. This will aid the identification of the effective degrees of freedom underlying the resonance excitation of all states that couple to virtual photons.

V. OTHER TOPICS IN LIGHT QUARK BARYON SPECTROSCOPY THAT ARE ADDRESSED WITH THIS LOI.

Besides the search for hybrid baryon states, there are many open question in our knowledge of the structure of ordinary (non-gluonic) baryon excitations, that can be addressed with data coning from the same experiment and taken in parallel with it. As an example we show in Fig. 10 the electrocouplings of the $N(1680)\frac{5}{2}^+$ resonance, the strongest state in the third nucleon resonance region. With the exception of the real photon point, the data are quite sparse for $Q^2 \leq 1.8\text{GeV}^2$ and the extremely high statistics data expected from this intended project could address many of these questions. Note that the high Q^2 part will be covered by the approved JLab experiment E12-09-003. An even more compelling example is the $N(1675)\frac{5}{2}^-$ state where data at $Q^2 > 1.8\text{GeV}^2$ have been published recently by the CLAS collaboration [16]. Figure 11 shows the currently available helicity amplitudes. The low Q^2 data are very important as for this state any non-zero values of the electro-coupling amplitudes will measures the strength of the meson-baryon contributions as the quark transitions are strongly suppressed by the Moorhouse selection rule. The main data needed are single pion production $ep \rightarrow e'\pi^+n$ and $ep \rightarrow e'\pi^0p$. These processes can be accumulated with sufficiently high event rate even with a pre-scale factor of 10 or more should the overall event rate be too high in this 2-prong topology.

VI. BEAMTIME ESTIMATE

The complete hybrid baryon program will require 3 beam energies at 6.6 GeV, 8.8 GeV, and 11 GeV to cover with highest statistics the lowest Q^2 range where the scattered electron is detected in the angle range from $2.5 \leq \theta_e \leq 4.5\text{deg}$. For the proposal we will likely request new beam time of 60 days that is divided into 20 days at 6.6 GeV, and 40 days at 8.8 GeV. The 11 GeV data of 60 days will be taken simultaneously with the already approved experiment E12-11-005.

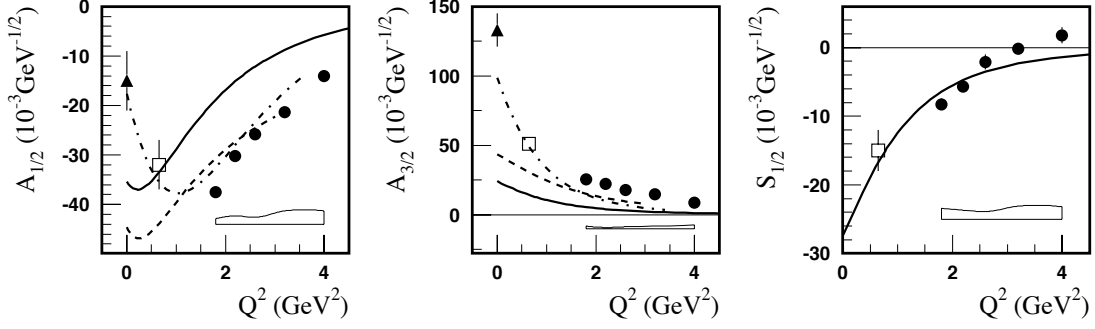


FIG. 10: Electrocoupling amplitudes of the $N(1680)_{\frac{1}{2}}^{5+}$ resonance.

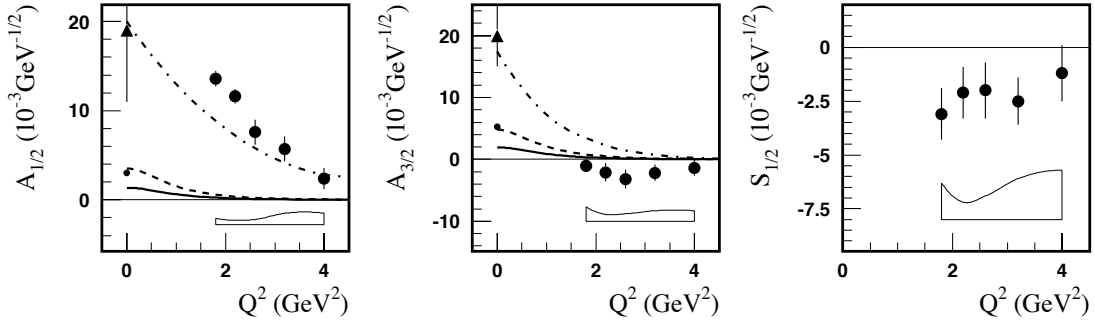


FIG. 11: Electrocoupling amplitudes of the $N(1675)_{\frac{1}{2}}^{5-}$ resonance. Quark models predict the transverse amplitudes to be suppressed. The significant deviation of the $A_{1/2}$ amplitudes is consistent with meson-baryon contributions to the excitation strength (dashed-dotted lines).

VII. SUMMARY

In this letter we discussed an extensive program to study the excitation of nucleon resonances in meson electroproduction using electron beam of 6.6, 8.8, and 11 GeV energy. The main focus is on the search for gluonic excitations of light-quark baryons in the mass range up to 3.5 GeV, and in the range of Q^2 from 0.05 to 2.0 GeV^2 . We have estimated the rates for two of the channels we propose to study, $K^+\Lambda$ ($K^+\Sigma$) and $p\pi^+i\pi^-$, but all other channels detected in CLAS12 will be subjected to analyses as well. The expected rates are very high, thanks to the very forward scattered electrons with minimum $Q^2 = 0.05 \text{ GeV}^2$ that are detected in the Forward Tagger. The data will be subjected to state-of-the-art partial wave analyses that were developed during the past years for baryon resonance analyses. Beyond the main focus of the LOI on hybrid baryons, a wealth of data will be collected in many different channels that will put meson electroproduction data on par with real photo production in terms of production rates and allow for the vast extension of the ongoing N^* electroexcitation program with CLAS at lower energies.

-
- [1] K. A. Olive *et al.* [Particle Data Group Collaboration], Chin. Phys. C **38**, 090001 (2014)
 - [2] Z. p. Li, V. Burkert and Z. j. Li, Phys. Rev. D **46**, 70 (1992).
 - [3] I. G. Aznauryan *et al.* [CLAS Collaboration], Phys. Rev. C **78**, 045209 (2008) [arXiv:0804.0447 [nucl-ex]].
 - [4] I. G. Aznauryan *et al.* [CLAS Collaboration], Phys. Rev. C **80**, 055203 (2009) [arXiv:0909.2349 [nucl-ex]].
 - [5] I. G. Aznauryan and V. D. Burkert, Prog. Part. Nucl. Phys. **67**, 1 (2012) [arXiv:1109.1720 [hep-ph]].
 - [6] T. Barnes and F. E. Close, Phys. Lett. B **123**, 89 (1983); E. Golowich, E. Haqq, and G. Karl, Phys. Rev. D **28**, 160 (1983); C.E. Carlson and T.H. Hansson, Phys. Lett. B **128**, 95 (1983); I. Duck and E. Umland, Phys. Lett. B **128** (1983) 221.
 - [7] S. Capstick and P. R. Page, Phys. Rev. C **66**, 065204 (2002), [nucl-th/9904041]; Phys. Rev. D **60**, 111501 (1999), [nucl-th/0207027].
 - [8] P. R. Page, Int. J. Mod. Phys. A **20**, 1791 (2005) [nucl-th/0410084].
 - [9] C. E. Carlson and N. C. Mukhopadhyay, Phys. Rev. Lett. **67**, 3745 (1991).

- [10] T. T. Takahashi and H. Suganuma, Phys. Rev. Lett. **90**, 182001 (2003) [hep-lat/0210024].
- [11] C. K. Chow, D. Pirjol and T. M. Yan, Phys. Rev. D **59**, 056002 (1999) [hep-ph/9807387].
- [12] J. J. Dudek and R. G. Edwards, Phys. Rev. D **85**, 054016 (2012) [arXiv:1201.2349 [hep-ph]].
- [13] N. Suzuki, B. Julia-Diaz, H. Kamano, T.-S. H. Lee, A. Matsuyama and T. Sato, Phys. Rev. Lett. **104**, 042302 (2010) [arXiv:0909.1356 [nucl-th]].
- [14] Z. P. Li, Phys. Rev. D **44**, 2841 (1991).
- [15] Z. P. Li, V. Burkert and Z. J. Li, Phys. Rev. D **46**, 70 (1992).
- [16] K. Park *et al.* [CLAS Collaboration], arXiv:1412.0274 [nucl-ex].
- [17] T. Corthals, D. G. Ireland, T. Van Cauteran and J. Ryckebusch, Phys. Rev. C **75**, 045204 (2007) [nucl-th/0612085].
- [18] L. De Cruz, J. Ryckebusch, T. Vrancx and P. Vancraeyveld, Phys. Rev. C **86**, 015212 (2012) [arXiv:1205.2195 [nucl-th]].